

Wavefront control of large optical systems

Aden B. Meinel, Marjorie P. Meinel and J. B. Breckinridge

Jet Propulsion Laboratory, California Institute of Technology
4800 Oak Grove Drive, Pasadena, CA 91109, USA

ABSTRACT

Several levels of wavefront control are necessary for the optimum performance of very large telescopes, especially segmented ones like the Large Deployable Reflector. In general the major contributors to wavefront error are the segments of the large primary mirror. Wavefront control at the largest optical surface may not be the optimum choice because of the mass and inaccessibility of the elements of this surface that require upgrading. The concept of two-stage optics was developed to permit a poor wavefront from the large optics to be upgraded by means of a wavefront corrector at a small exit pupil of the system.

1. INTRODUCTION

The concept for a 20 to 30 meter diameter far infrared (FIR) and submillimeter (SMM) telescope, termed Large Deployable Reflector (LDR), was the topic at the 1982 NASA conference at Asilomar, California. It early became apparent that packaging of the primary mirror, its wavefront sensors, lock-on sensors and control actuators into a deployable or assembleable system posed severe or unsolvable engineering challenges as well as the prospect of LDR being unaffordable even if solutions were found. We, in collaboration with J. Stacy, developed a concept^{1,2} that utilized a passive primary and that made all wavefront corrections to achieve diffraction-limited performance by means of a small active segmented mirror located at an exit pupil. This concept is termed "two-stage optics" and is illustrated in Fig. 1.

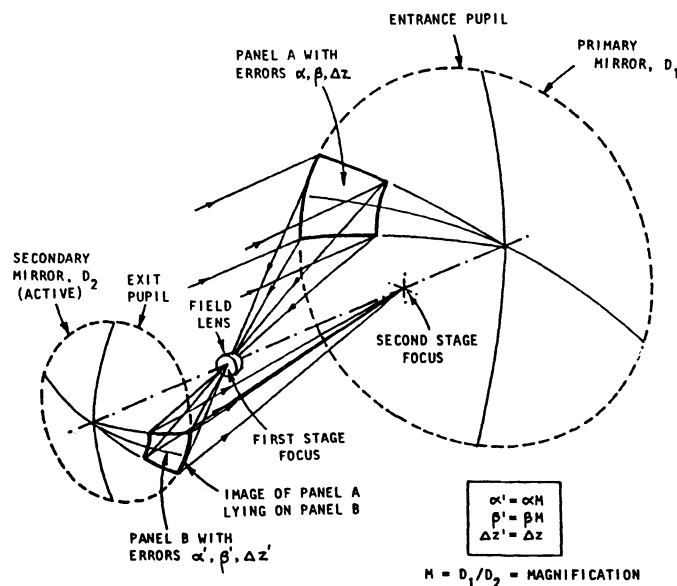


Fig. 1. Generalized diagram of a two-stage optical system showing a typical panel of the segmented primary mirror which is imaged by a field lens upon an identical, but minified, panel on the second mirror. For proper operation the image of the primary panel must exactly coincide in three dimensional space with the active panel in the second stage.

2. TWO-STAGE OPTICS CONCEPT

2.1. Functional scheme

Two-stage optics³ is defined as a first stage that consists of large optics which form an approximate image followed by a second stage which produces a high resolution image. As embodied in the LDR the errors of tip, tilt and piston, as well as surface figure errors of each segment, can be corrected by means of minified segments located at an exit pupil in the second stage. Wavefront correction in a second stage can manage wavefront errors as large as one thousand times greater than diffraction-limited requirements. The field element between the first and second stages, shown as a lens in Fig. 1, must be large enough to gather all the rays arriving at the first focus and, in addition, be enough oversized to provide the field of view desired for the system. The fourth element, located at the image of the primary mirror, is provided with the opposite wavefront error of the primary, and the net result is that the wavefront error is reduced to zero.

2.2. Corrector location

In principle one can place a wavefront corrector at any place in the optical train and achieve diffraction-limited performance for the on-axis image. The location of the correction of the primary at the image of the primary, i.e. the exit pupil, permits correction over a large field of view. The size of the field of view depends on the magnitude of the wavefront errors and the minification factor M of the second stage, as discussed below.

2.3. LDR configuration

Six configurations evaluated for LDR are shown in Fig. 2. Option 1 is a traditional 2-mirror Cass. Option 2 is the basic four-mirror, two stage configuration. Several alternate options are also shown that will be discussed below.

The basic excellence of this four-mirror system has been shown by D. Korsch and others. One can even use a spherical primary and secondary when the primary focal ratio is as slow as $F/2$. For LDR and typical compact IR and SMM telescopes the primary focal ratio is between $F/0.35$ and $F/0.8$. The four-mirror configuration in these cases requires an aspheric primary and secondary, as well as an aspheric tertiary.

Fig. 3 illustrates the advantage of two-stage optics in simplifying the control of a large segmented mirror telescope and reducing its cost by having all of the active components pre-assembled in a monolithic module. In this case, the adaptive quaternary mirror is a 1 meter hexagonal monolithic element, which is shown standing beside the 20-m diameter primary. Reliability and the prospect for lowering system cost is enhanced by use of a pre-assembled array of segments. Each hexagonal segment on the quaternary is accurately scaled to $1/20$ th the size of the primary segments.

Options 4 through 6 place the second stage behind the primary mirror as shown in Fig. 2. We have evaluated a design of this type in which the quaternary is only 50 cm diameter. In this case each segment of the quaternary is only 50 mm across.

2.4. Segment location

Each quaternary segment is placed at the image of each corresponding segment of the primary. This means that the surface error of each segment can be corrected by placing the inverse surface error on its corresponding image segment. This relationship reduces the manufacturing tolerance on each primary segment and hence has a beneficial impact on segment cost. One can further make the quaternary segment adaptive in order to allow real time on-orbit correction of the primary segment figure.

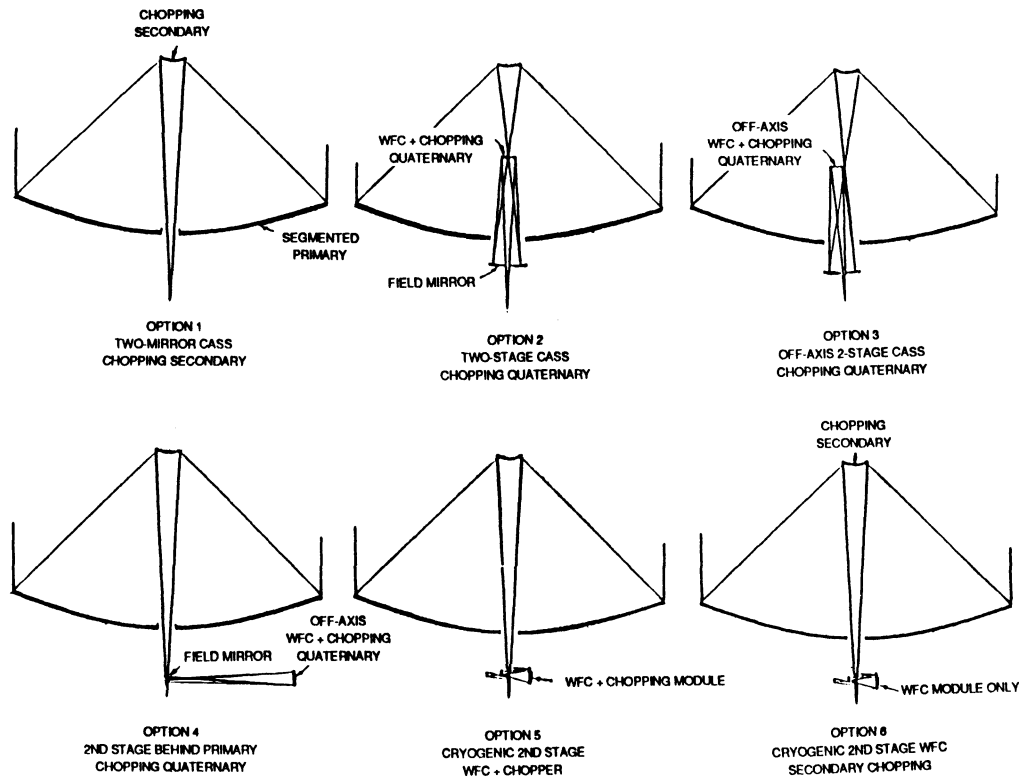


Fig. 2. Six configuration options evaluated for the LDR. Option 1 is a single stage configuration, while Options 2 through 6 are two-stage configurations. For practical considerations, placing the second stage within a cryogenic zone is attractive in a far infrared / submillimeter telescope.

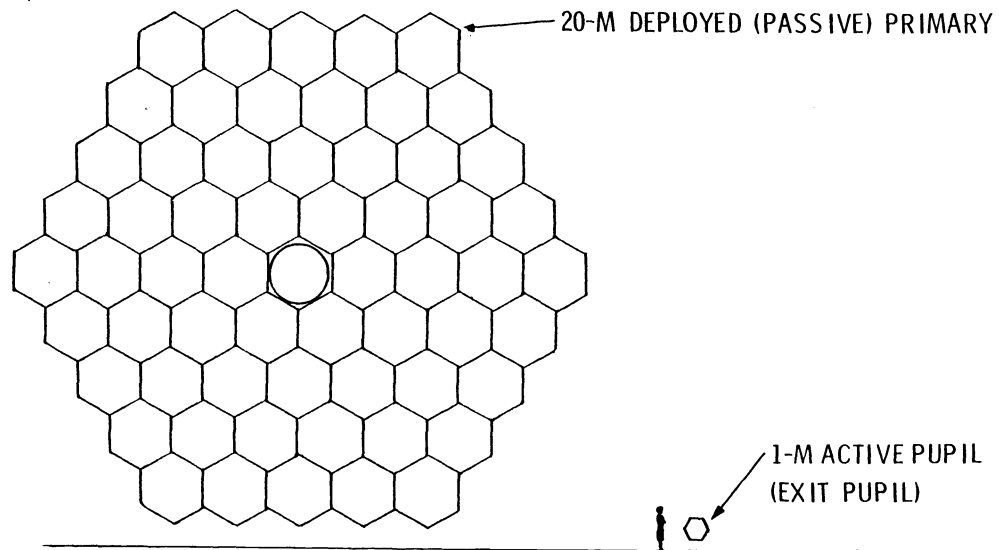


Fig. 3. The dramatic reduction in size of the active portion of a segmented mirror achieved by placing the active components in a minified second stage is illustrated for the case of a 20-m LDR.

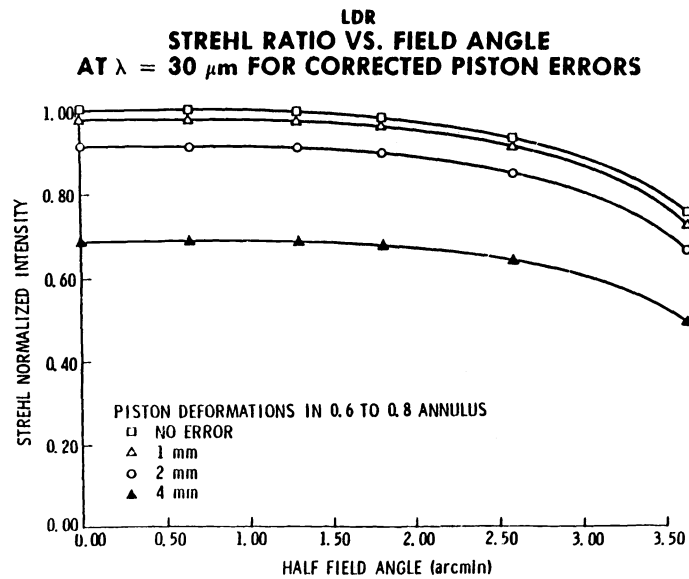


Fig. 4. Variation of the Strehl ratio for LDR when piston errors are corrected by compensating piston displacement of a segment in the second stage is illustrated. Note that correction is essentially perfect for 1 mm piston errors.

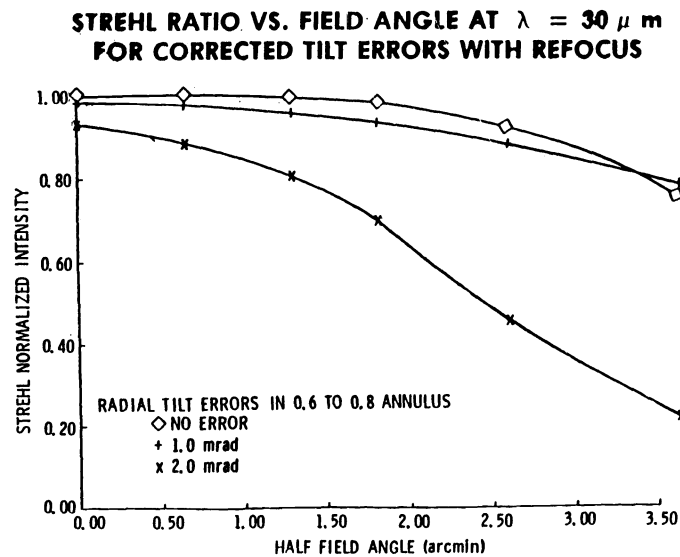


Fig. 5. Variation of the Strehl ratio for LDR when tilt errors are corrected by compensating tilts of a segment in the second stage is illustrated. Note that a 1 mrad error is essentially perfectly corrected.

2.5. Error sensing

In order to control the quaternary the error of the system must be sensed. This means that the phasing must be examined using a reference star or an onboard retroreflector system to show changes in the optical path. In this regard wavefront sensing of a basic Cassegrain LDR and a two-stage LDR are identical. The main difference is in the location and size of the actuators and associated sensing and control subsystems. As for size, a typical segment would use a 100 mm span hexagon mounted on a three-degrees-of-freedom set of three actuators, providing the basic three-degrees of freedom. This small size is very similar to that used in the US Air Force Weapons Laboratory wide-field MMT⁴.

3. ANALYSIS

3.1. LDR configuration analysis

Computer modeling by J. Stacy¹ of the design in Fig. 2 showed that diffraction-limited performance could be obtained over a field of view of 10 arcmin diameter with segment piston errors of 1 millimeter. Fig. 4 shows the Strehl ratio as a function of field angle for several levels of piston error, while Fig. 5 shows the Strehl ratio as a function of tilt angle. Note that the degree of correction is excellent even with errors that are larger than will probably be the case for a deployed or assembled LDR.

3.2. Generalized analysis

The Meinels explored the parametric performance of generalized two-stage optics as a function of demagnification of the second stage, the improvement factor, and the resulting field of view. Fig. 6 shows how the performance depends on these two factors for several variants of two-stage optics. This Figure shows that if very wide field performance of several degrees is required the allowable demagnification factor M is small for a given improvement factor Q. Fig. 7 shows the performance on other scales of use in design decisions. Analysis of several primary focal ratios and configurations shows the same approximate relationship between field angle M and Q.

3.3. Field of view

The geometric effect that causes a limitation in the field over which piston errors can be corrected is illustrated in Fig. 8. The off-axis object ray angle is multiplied by the factor M. This means that the ray path length for a unit piston error at the quaternary is multiplied by $\Delta z / \cos M\theta$, whereas it should have been $\Delta z / \cos \theta$.

4. ISSUES AND LIMITATIONS

4.1. Thermal emission

In order to optimize performance of a passive FIR / SMM telescope it is essential that thermal emission from the telescope mirrors be minimized. Adding two additional surfaces of the second stage, therefore, increases this background. The small size of the second stage, however, means that it can in principle be placed close to the cryogenic instrumentation package and be actively cooled by blowdown from the cryogenic stage. Several configurations involving Cassegrain re-imaging components have been developed that fold the second stage into a package less than 3 meters in transverse width and fit well into the cryogenic zone.

4.2. Chopping

Chopping is currently the mode whereby astronomers correct for slow variations in the background signal and detector noise. This procedure involves pointing a few arcminutes off the observation target. For small

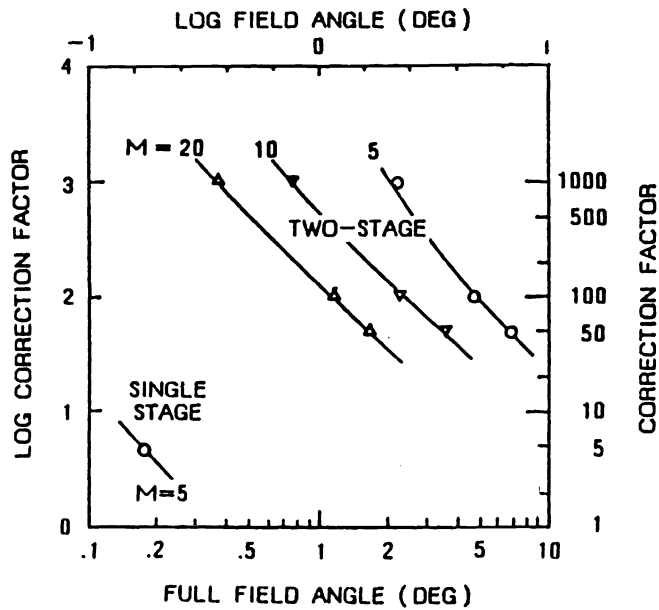
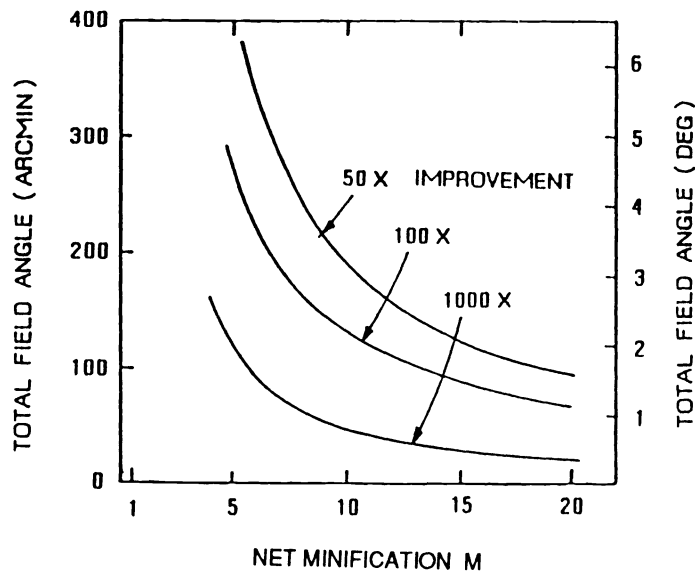


Fig. 6. Dependence of the correction factor possible in the second stage as a function of the minification factor M and desired full field angle, showing that significant fields can be corrected for errors large enough to have otherwise rendered the system useless.

IMPROVEMENT vs NET MAGNIFICATION

- ERROR BALANCED, CENTER = EDGE



EXAMPLES: 1000 X : 200 ASEC DIA IMAGE \rightarrow 0.2 ASEC IMAGE
 100 X : 20 ASEC DIA IMAGE \rightarrow 0.2 ASEC IMAGE

Fig. 7. The dependence of field angle as a function of the minification factor M for given values of improvement in the wavefront error is illustrated.

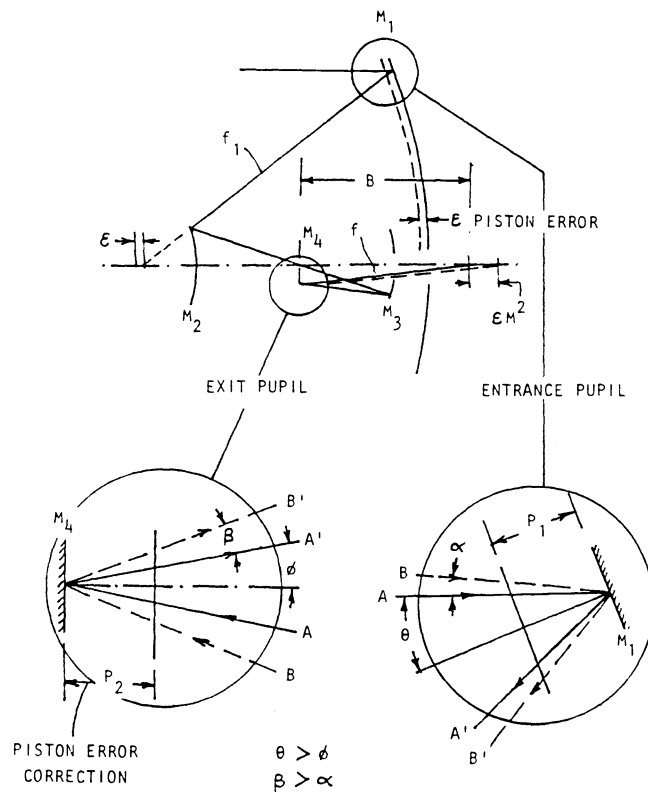


Fig. 8. Geometry for a four-mirror two-stage configuration having a piston error on one panel of the primary. The major residuals are the focus position change and the residual caused by the larger cosine value for the angle beta compared to the angle alpha, illustrated in the lower two diagrams.

telescopes it can be done by moving the entire telescope, but for large ones it is done by chopping the Cass secondary. The result of chopping the secondary is that the beam (or feed pattern) moves on the primary mirror. If either dust or a temperature gradient is present on the primary a false modulation results, which sets allowable limits on both cleanliness and transverse ΔT . Variants of the basic four-mirror LDR that place the second stage, wavefront correction (WFC) and chopping at other locations are shown in Options 3 through 6 in Fig. 2.

4.3. Beam motion

In the case of two-stage optics one can do the chopping at some other optical surface than the secondary. If it is at the quaternary, which is at an image of the primary, no beam motion will occur on the primary, greatly relaxing requirements on the transverse thermal gradient ΔT . The beam will, however, move on both the secondary and tertiary mirrors, which places requirements on their values of ΔT and cleanliness. There will be no beam motion on any other optical surface between the chopping mirror and the instrument detector.

4.4. Diffraction spillover

At SMM wavelengths diffraction spillover could become a problem when the reduction factor M becomes large. The image of each primary segment at the quaternary will have a diffraction edge as illustrated in Fig. 8. We have evaluated the issue of diffraction spillover for the case where the quaternary mirror is 1/40th the 20 m diameter of the primary mirror, or 50 cm across ($M = 40$). Each 2-meter primary segment thus has a quaternary segment of only 50 mm dimension.

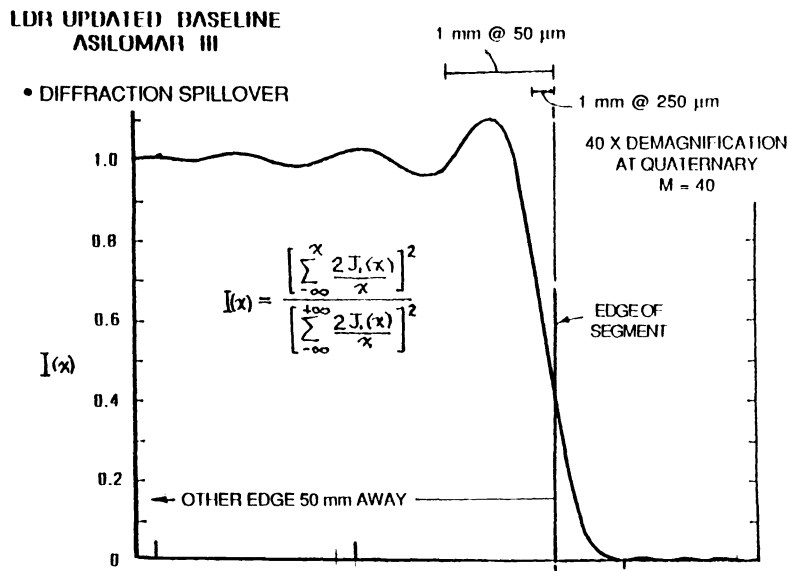


Fig. 9. Diffraction spillover at the edge of the image of a primary segment at the minified second stage segment for a case of minification factor 40 and for two wavelengths as indicated by the length of the lines at the upper right. The fractional amount of spillover is very small.

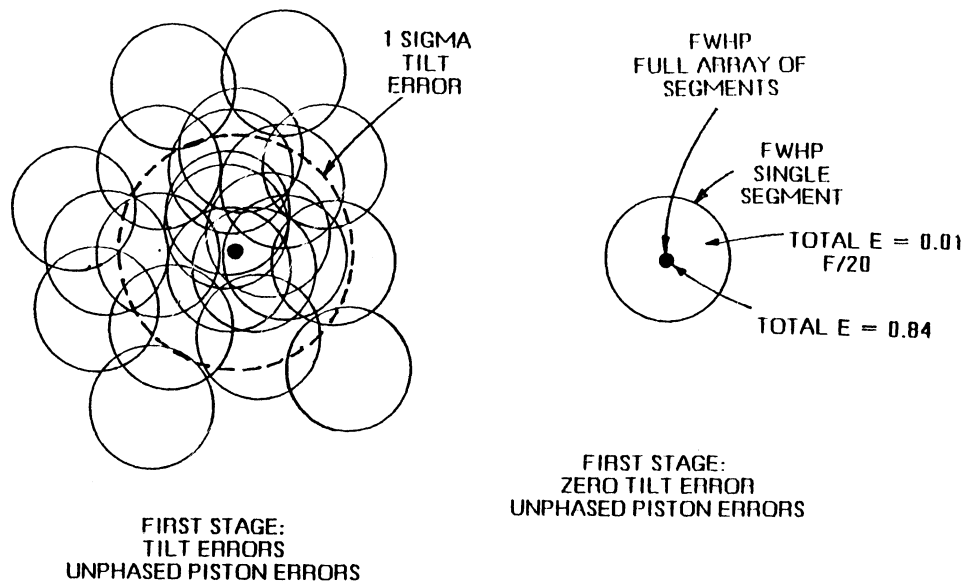


Fig. 10. The resultant image shape at the final two-stage focus for the case where the primary segments have both piston and tilt errors (left), and for the worst case where the tilt errors are zero (right). The relative diameters of the spillover diffraction disc and the central image are 10:1; thus the energy of the spillover image received by a feed is diluted by a factor of 100.

- WORST CASE: ZERO TILT ERROR (ALL SPILLOVER IMAGES OVERLAP)

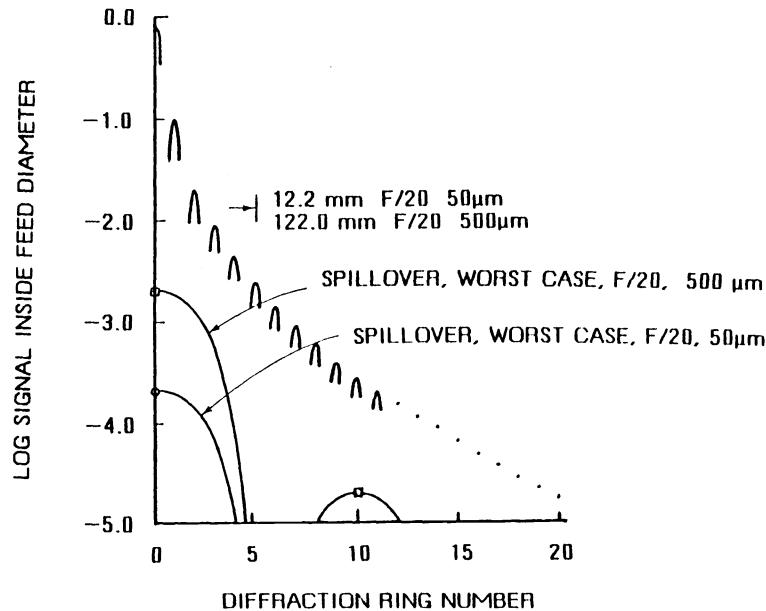


Fig. 11. Graph of the signal received by a feed of diameter equal to the full width half power (FWHP) of the central image, showing that the diffraction ring signal from the core image is much larger than the signal from the spillover energy (for both 50 μm and 500 μm wavelengths).

The linear spread of the diffraction pattern of Fig. 9 is a function of wavelength. The length of the line at top right shows the length of 1 mm for wavelengths of 50 μm and 250 μm . Note that the other edge of the quaternary segment is 50 mm away to the left. The fraction of the total flux imaged on a segment lying beyond the edge of the segment is 0.42% at 50 μm and 2.11% at 250 μm .

This diffraction spillover will not be corrected for the piston error of the two segments involved. This means that the spillover of all the segments will be mutually unphased and hence spread over a diffraction pattern 20 times larger than the phased diffraction pattern of the segment mirror array, as illustrated in Fig. 10 (right). These percentages spread over the larger circle mean that the signal seen by the feed (which is approximately the diameter of the small circle) is only 1×10^{-5} @ 50 μm and 5×10^{-5} @ 250 μm , which is very small indeed.

Fig. 11 shows the spillover signal relative to the diffraction maxima of the phased portion of the system. Note that in general it lies one to two orders of magnitude below the diffraction maxima.

Inasmuch as the segments will in general have tilt errors as well as phase errors the spillover radiation is even more widely spread in the focal plane because of segment tilts. Fig. 10 (left) shows the case with tilt errors. Clearly the amount of spillover radiation detected with a feed the size of the black dot will be smaller than 1×10^{-5} even at 250 μm .

4.5. Chopping angle

Chopping of the quaternary is bounded by the motion of the beam at the first stage focus. The object does not move in the first focus. The sample point moves to a nearby region of the sky. This means that the size of the hole in the quaternary limits the chopping angle as well as the maximum tip error of the first stage. To make this field larger we have the option of placing the quaternary off the optical axis as illustrated in Fig. 2, Option 3.

5. SYSTEM DESIGN CHOICES

5.1. One-stage or two-stage optics?

The critical factor in deciding whether LDR should use two-stage optics is whether it will be satisfactory from the viewpoint of the astronomer. Since no terrestrial FIR telescope uses two-stage optics there is no practical experience in how it performs, and hence there is some uneasiness that some unanticipated problem will be discovered. The obvious answer to this apprehension is to test the technique on a ground-based or airborne FIR telescope. Such a test seems to be imperative because the cost of LDR could be much lower and reliability greater through elimination of active segments on the primary .

5.2. Which element is chopped?

Since the beam is stationary at optical surfaces between the chopped mirror and the detector one can chop ahead of the wavefront controlling surface. This would avoid chopping an element that has a lot of associated hardware and sensors, and thus more mass, than if chopping were the only function. We therefore recommend a separate chopping mirror ahead of the wavefront control mirror. We have explored several designs in which this is accomplished within a compact optical package associated within the cryogenic zone of LDR.

5.3. Is attachment of passive primary panels advantageous?

Attachment of panels to the nodes of the backup structure is an area where conceptual design work has been directed to the case where all of the actuators and sensors are integrated components. The result has been a very complex system distributed over the several meter span of the primary segments. In principal a much simpler attachment and handling subsystem can be developed if the segments are passive and can be attached with phasing errors between the adjacent corners of a panel attaching to the same node within a few microns through manufacturing dimensional quality control.

5.4. Can collimation errors also be corrected?

In principal both decollimation coma and fine guiding errors can be corrected by the active quaternary. We do not recommend doing so for three practical reasons:

1. Applying these corrections subtracts from the dynamic range for control of wavefront errors from the optical surfaces of the system.
2. It is much easier to correct both focus and decollimation coma by providing three axial screws to correct focus by simultaneous motion of all three or to correct coma by motion of any two.
3. Fine guiding can be better accomplished by tilting the secondary or by moving the entire telescope.

6. STATUS

6.1. PSR program

At present the Precision Segmented Reflector (PSR) testbed program is directed toward active primary mirror segments, not the two-stage optics option. It is generally agreed that use of a basic two-mirror Cassegrain is simpler if the problems of attachment and control of full-sized segments are demonstrated to be adequate. The current two-stage design is par-focal with the standard Cass design. This means that a second stage module can be added to the PSR testbed at any time so that the tradeoffs between the two choices can be evaluated.

6.2. Angel 32-m terrestrial segmented telescope

Angel⁵ has proposed tiling a 32-m radio telescope-type dish with small segments, each about the size of the atmospheric structural parameter r_0 . This means segments of the order of 20-cm-span

hexagons. These segments can be pre-phased in attachment to common nodes of the backup structure. The entire array will then deform as the backup structure deforms. One can in this case use a continuous deformable wafefront control surface at a second-stage exit pupil to keep the entire 32-m array properly phased to the degree necessary for speckle imaging.

7. ACKNOWLEDGEMENT

The research described in this paper was carried out by the Jet Propulsion Laboratory, California Institute of Technology, under a contract with the National Aeronautics and Space Administration.

8. REFERENCES

1. JPL Report, LDR Asilomar 2 (1985).
2. US Patent No. 4,836,666.
3. A. B. Meinel and M. P. Meinel, "Limits to size for terrestrial telescopes: two-stage optics," *SPIE Advanced Technology Optical Telescopes III*, Vol 628, p 472 (1986).
4. C. DeHainaut, "Four telescope phased array optical simulation," *SPIE's 1990 astronomical telescopes and instrumentation for the 21st century* (in press).
5. R. Angel, "Filled aperture telescopes in the next millennium," *SPIE's 1990 astronomical telescopes and instrumentation for the 21st century* (in press).